Turk J Phys
28 (2004) , 41 – 48.

AC conductivity and Dielectric Study of Chalcogenide Glasses of Se-Te-Ge System

Fathy SALMAN
Physics Department, Faculty of Science, Benha-EGYPT

Received 03.04.2003

Abstract

The ac conductivity and dielectric properties of glassy system $Se_xTe_{79-x}Ge_{21}$, with x = 11, 14, 17 at.%, has been studied at temperatures 300 to 450 K and over a wide range of frequencies (50 Hz to 500 kHz). Experimental results indicate that the ac conductivity and the dielectric constants depend on temperature, frequency and Se content. The conductivity as a function of frequency exhibited two components: dc conductivity σ_{dc}, and ac conductivity σ_{ac}, where $\sigma_{ac} \sim \omega^s$. The mechanism of ac conductivity can be reasonably interpreted in terms of the correlated barrier hopping model (CBH). The activation energies are estimated and discussed. The dependence of ac conductivity and dielectric constants on the Se content x can be interpreted as the effect of Se fraction on the positional disorder. The impedance plot at each temperature appeared as a semicircle passes through the origin. Each semicircle is represented by an equivalent circuit of parallel resistance R_b and capacitance C_b.

1. Introduction

Measurement of AC conductivity of amorphous chalcogenide semiconductors has been extensively used to understand the conduction process in these materials [1]. The electrical properties of Se-based glasses are very interesting, for these materials exhibit effects such as optical memory and photo darkening [2, 3] to which the study of their electrical behavior could shed light. Generally, the undoped chalcogenide glasses show low values of electrical conductivity, which could mean a serious limit to their technological application and electrical measurements. Certain additives are used to improve these properties. Enormous interest has been shown in Selenium-tellurium alloys due to their great hardness, higher photosensitivity, higher crystallization temperature and smaller aging effects as compared to pure amorphous Se [4]. Addition of germanium to the Se-Te system causes structural changes in the material which in turn modify band structure, and hence the electrical properties of the material.

The aim of this study is to report some electrical features, and determine the influence of Selenium content on the electrical conductivity of the Ge-Te-Se system and characterize its dependence on temperature. The study focuses on three samples of $Ge_{21}Te_{79-x}Se_x$ composition: x = 11, 14, 17 at% (the respective samples denoted by S_1, S_2 and S_3). That is, the Te part of the Ge-Te content is substituted by Se, with the Ge set at a fixed content. As of concern in the study is the characterization of the dielectric behavior.

To establish a picture of the conduction mechanism, complex impedance analysis is used [5, 6]. The dependence of impedance on both frequency and temperature has been investigated. The complex impedance is considered as a contribution of both real (z') and imaginary (z'') parts and is written in the form $z^* = z' - jz''$. The frequency dependence of both components of the impedance permits separation of the sample resistance for the grain bulk, R_b.

2. Experimental Work

$Ge_{21}Te_{79-x}Se_x$ samples, with x = 11, 14, 17 at% (and denoted as samples S_1, S_2 and S_3, respectively) were prepared on the basis of the percentage atomic composition. High purity elements (99.999%) of the desired fractions were mixed together in a silica ampoule 20 cm long, 1 cm diameter and of 2 mm wall thickness. The ampoules were heated in a Heraeus Ks 120 muffle furnace (with the ability to heat to the maximum temperature of 1200 ± 20 °C). Ampoules were heated for 6 hours at a temperature of 1200 °C with continuous shaking to ensure good homogeneity. The ampoules, kept horizontally, were then quenched in ice-water to ensure constant cooling rate. Samples as small discs of thickness ∼0.05 cm were produced. The measurements were carried out on bulk samples of uniform discs from the sintered ingot. Each disc has a thickness equal to about 0.05 cm and a diameter equal to about 1.0 cm. Good contact was attained by painting both faces of the sample disc with air-drying conducting silver paste.

The bulk density D_b of the prepared samples was measured using Toluene as an immersing medium. Results show that the value of bulk density depends on the composition, mainly on the Te-content. Bulk density of the samples is given in Table 1. X-ray diffractograms of all prepared samples showed the samples to be amorphous. The DTA (differential thermal analysis) thermograms of samples belonging to these three samples were recorded to detect the glass transition temperature T_g (see Table 1).

Table 1. Composition, Density, D_b, and glass transition temperature T_g for the three glassy alloys under study.

	Composition			Db.	Tg
Sample No.	Ge	Te	Se	Gm/cm^2	C.
1	21	68	11	5.40	151
2	21	65	14	5.46	150
3	21	62	17	5.51	153

The impedance, in terms of modulus $|z|$ and phase angle ϕ, was measured using a TESLA BM 507 impedance meter, in the frequency range 50 Hz–500 kHz and at various temperatures. The temperatures were chosen from the range 300–420 K. The resistance R and capacitance C are computed via the established relationships: $R = |z|/\cos\phi$ and $C = \sin\phi \,/\, \omega|z|$, where ω is the angular frequency. The ac conductivity has been calculated by the relation $\sigma_{ac} = 1/R \cdot \quad t/A$, where t and A are the thickness and cross-sectional area of the sample, respectively.

3. Results and Discussion

3.1. Frequency dependence of conductivity

Figure 1 shows the total measured conductivity as a function of frequency $\sigma_{tot}(\omega)$ in the frequency range 50 Hz–500 kHz at various temperatures in the range 300–420 K, for sample S_2, chosen as an example of a typical Ge-Te-Se glass. The conductivity behavior can be divided according to the measured frequency. In the low frequencies region, the conductivity is constant and is taken to be the dc conductivity σ_{dc}. Theoretically, this behavior may be modeled by transport taking place through infinite random free-energy barriers [7]. When the frequency is increased, the conductivity is found to obey a power relation, $\sigma_{ac} \sim \omega^s$, where s is a function of temperature. Such behavior may be modeled as transport is dominated by conduction hopping through infinite clusters [7]. The crossover frequency from σ_{dc} to $\sigma_{ac}$is the frequency of peak of dielectric loss, and increases with temperature. At higher frequencies, the conductivity tends to stability. At higher temperature, the curve of log σ_{tot} vs. log f becomes nearly linear, behavior which may be dc conduction. The other compositions also indicate a similar dependency.

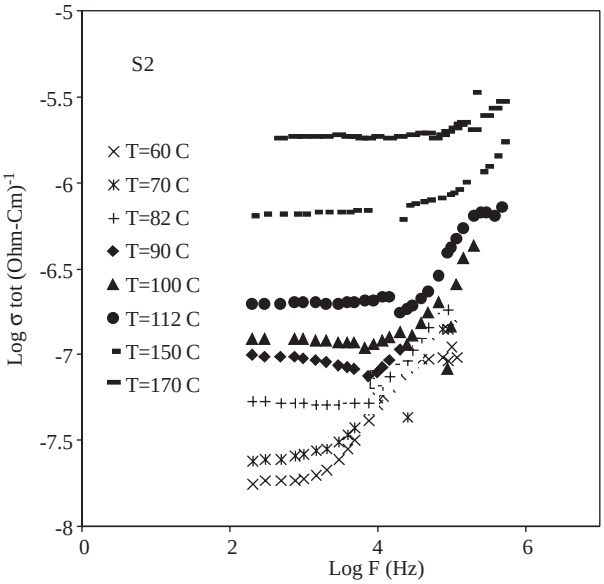

Figure 1. The total conductivity as a function of frequency at different temperatures for sample S_2.

Hence, the total conductivity is a sum of the two components: dc conductivity σ_{dc}, which is independent of frequency; and frequency dependent conductivity σ_{ac}, i.e.

$$\sigma_{\rm tot}(\omega) = \sigma_{dc} + \sigma_{ac}. \tag{1}$$

The values of σ_{dc} are obtained by extrapolating $\sigma_{tot}(\omega)$ to $\omega = 0$, and plotted as a function of the reciprocal of temperature for each sample. The behavior of $\log(\sigma_{dc})$ vs. $1/T$ for the three compositions S_1, S_2 and S_3 is presented in Figure 2. These Arrhenius plots of the dc conductivities reveals the activation energies E_{dc} as listed in Table 2. One may note that S_1 ($Tg = 424$ K) exhibits a higher conductivity curve than for samples S_3($Tg = 426$ K) and S_2 ($Tg = 423$ K). The curve of conductivity for each sample seemed to be related to the temperature of the glass transition T_g obtained from DTA measurements (see Table 1). This reflects a change in the structure of the glass matrix, which in turn affects the electrical conductivity.

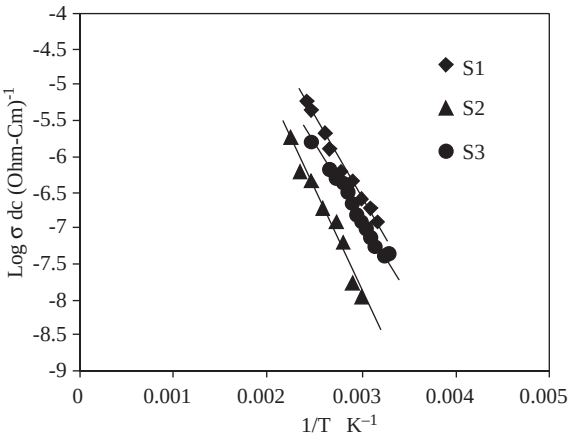

Figure 2. The dc conductivity as a function of reciprocal of temperature for samples S_1, S_2 and S_3.

Values of frequency exponent s is plotted against temperature T, for each composition of the Se-Te-Ge system, and shown in Figure 3. Each curve in this figure shows a decrease in the exponent s with an increase of the temperature, showing that s is temperature-dependent for each composition of the system. Thus the

experimental results agree with the correlated barrier hopping model (CBH), for a critical test of the CBH models comes from the temperature dependence of the ac conductivity and the frequency exponent [8].

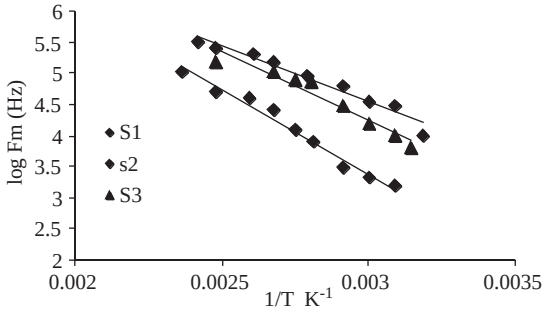

Figure 3. The temperature dependence of the exponent s for the investigated samples.

For the mechanism of ac conduction, the model of correlated barrier hopping (CBH) of bipolarons (i.e., two-electron hopping charged defects D^+ and D^-) has been proposed. According to the Guintini model, each pair of D^+ and D^- is assumed to form a dipole with relaxation energy E_r. This type of energy can be attributed to the existence of a potential barrier over which the carrier can hop. This observation leads to a decrease in the density of states due to the conversion of some bipolaron states (D^+, D^-) states into a single polaron state (D^o) according to the relation $(D^+) + (D^-) \rightarrow 2(D^o)$. The theory has explained many low temperature features, particularly the temperature dependant values of the parameters A and s. However, it does not explain the high temperature behavior so well, particularly in the low frequency range. Shimakawa [10] suggested that D^o states are produced by thermal excitation of D^+ and/or D^- states and that single polaron hopping (i.e. one-electron hopping between D^o and D^+ or D^-) contributes at high temperature. The temperature dependence of the crossover frequency f_m of the peaks of dielectric relaxation is shown in Figure 4. The plot of log f_m versus 1/T is found to be linear within the observable temperature and frequency ranges, so that we assume that f_m is given by a simple Arrhenius formula,

$$f_m = f_0 \exp(-E_r/kT), \tag{2}$$

where E_r is the activation energy of dielectric relaxation. As shown in Table 2, the activation energy, of both the dc conductivity and the dielectric relaxation is the same within experimental error, indicating that both ac conductivity at low frequency ($\omega\tau << 1$) and dc conductivity may occur by the same mechanism.

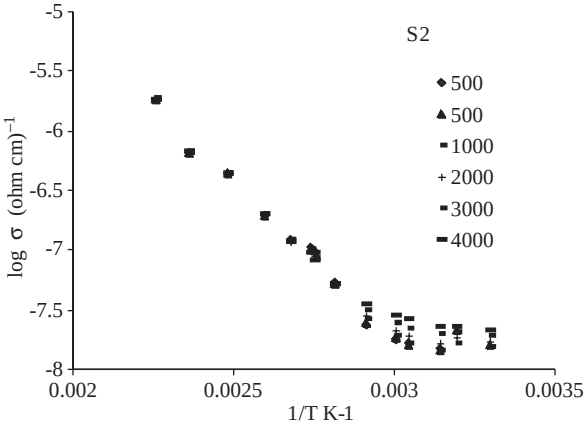

Figure 4. The temperature dependence of the frequency of the peak of dielectric relaxation for samples S_1, S_2 and S_3.

3.2. Temperature dependence of the conductivity $\sigma_{\text{tot:}}$

Figure 5 shows the total measured conductivity $\sigma_{tot}\ (\omega) = \sigma_{dc} + \sigma_{ac}$ as a function of reciprocal temperature at different frequencies, for sample S_2 chosen as an example. An Arrhenius plot of log σ vs 1/T is obtained with two different slopes at 1 KHz for each sample. It indicates two different thermally activated relaxation processes identified with translational jump diffusion and a localized reorientation motion of the carriers within a given neighborhood [11]. The conductivity in the first process at low temperature depends on frequency, while in the second process at high temperature is independent of frequency. The dependence of the electrical conductivity on temperature is then given by a typical Arrhenius-type relationship:

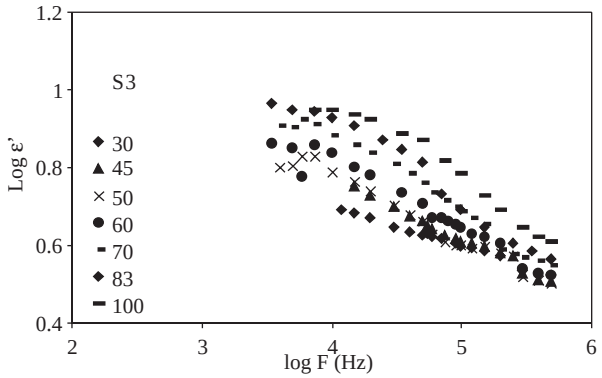

Figure 5. The temperature dependence of total conductivity at different frequencies for sample S_2.

$$\sigma_{tot} T = A \exp\left(-\frac{E_1}{kT}\right) + B \exp\left(-\frac{E_2}{kT}\right), \tag{3}$$

where A and B are constants, E_1 and E_2 are the high and low temperature activation energies and k is the Boltzmann constant. The values of E_1 and E_2 are reported in Table 2. It is noticed that the values of E_2 are nearly the same for all compositions whereas the values of E_1 depend on the composition. The high temperature activation energy E_1 values may be ascribed to the existence of defects, which are essentially the same in all our glasses.

3.3. Dielectric properties

Representative plots of dielectric constant $\varepsilon\prime$ and dielectric loss ε' versus frequency at different temperatures, as for example the S_3 glass sample, is shown in Figs. 6 and 7. The general features are the rapid decrease of $\varepsilon\prime$ and especially ε' with increasing frequency. Very large values of $\varepsilon\prime$ are observed, especially at high temperatures. Most of this behavior arises from electrode polarization effects [11–13].

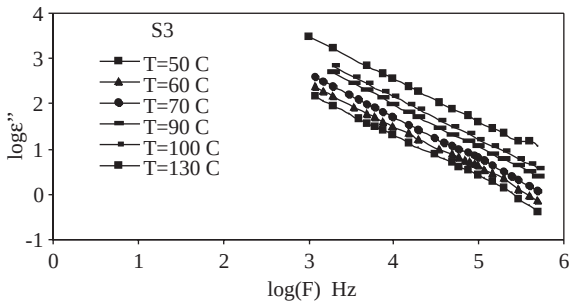

Figure 6. Frequency dependence of dielectric constant at different temperatures for sample S_3.

That $\varepsilon\prime$ depends significantly on temperature implies that the process responsible for the observed rise in $\varepsilon\prime$ is temperature-activated. No indication of a maximum is observed in ε'' in the region of frequency-dependent conductivity $\sigma_{ac}(\omega)$ (after accounting for dc conduction). This type of frequency dependence is commonly observed in chalcogenide glasses.

The observation of dielectric effects in the glasses implies that dipoles exist, corresponding to polaron hopping between sites of different energies, or polaron hopping about structural defects.

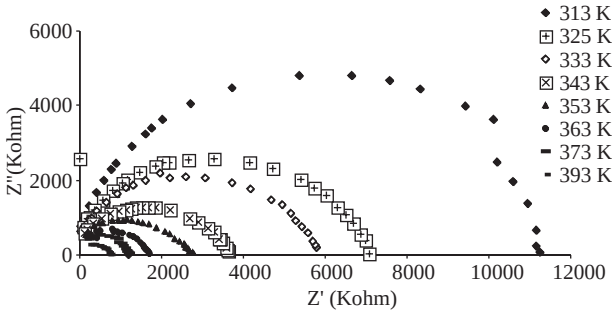

Figure 7. Frequency dependence of dielectric loss at different temperatures for sample S_3.

3.4. Bulk conductivity

The bulk conductivity for the glass system was measured using the complex impedance method [5]. The measurements were carried out in the temperature range 300–420 K and frequency range 50 Hz–500 kHz at various temperatures. The impedance plots for each sample appeared in the form of semicircles at the various temperatures. Plots of z' (the real part of the impedance) against z' (the imaginary part of the impedance) are shown for a typical glass sample, S_3, in Figure 8. Each semicircle has its center below z'-axis, begins from the origin at higher frequencies and ends at a point on the z'-axis, at lower frequencies. The intersection of the semicircle at lower frequencies ($\omega \cong 0$) with the z'-axis (the diameter) is taken as the sample bulk resistance R_b. The diameter of the semicircle drawn through the center from the origin makes an angle $\sim \pi/2$ with the z'- axis. It is also clear that the diameter of the semicircle decreases with increasing temperature, referring to the pronounced increase of dc conduction. The bulk conductivity has been calculated for all glasses samples and plotted as a function of temperature. Figure 9 shows the temperature dependence of the bulk conductivity for the three compositions S_1, S_2 and S_3. The activation energy is calculated and listed in Table 2.

Table 2. Composition and activation energies

Sample No.	Composition			E_1 eV	E_2 eV	Edc eV	E_r eV	E_b eV
	Ge	Te	Se					
1	21	68	11	0.42	0.20	0.44	0.35	0.43
2	21	65	14	0.50	0.25	0.56	0.44	0.43
3	21	62	17	0.36	0.10	0.42	0.53	0.36

These values of activation energy E_b are found to be close to the activation energy for the dc conductivity E_{dc} and dielectric relaxation E_r, respectively, indicating that the charge carrier has to overcome the same energy barrier while conducting as well as while relaxing, a behavior consistant with the fluctuation-dissipation theorem [13].

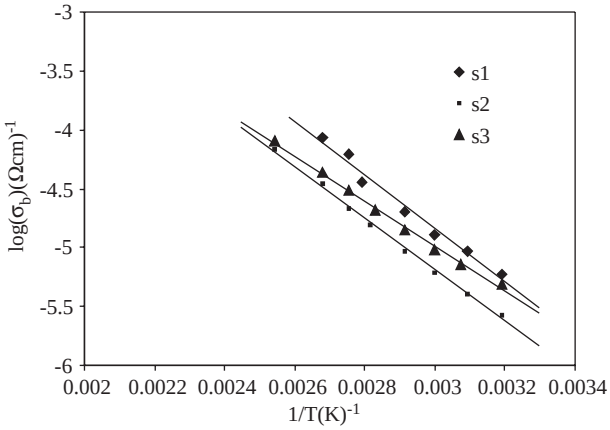

Figure 8. Impedance plots z'/z'' at different frequencies for sample S_3.

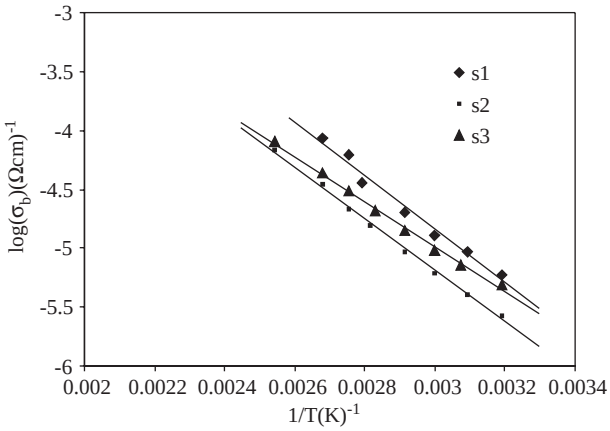

Figure 9. The temperature dependence of the bulk conductivity for the three compositions S_1, S_2 and S_3.

A typical impedance spectrum of the glass under study consists of a semicircle whose center lies just below the z'-axis. To fit this simple spectrum, an equivalent circuit consisting of a parallel combination of a resistance element R_b and a dispersive capacitance element $C_g(\omega)$ is proposed. R_b denotes the bulk resistance of the sample and C_g its geometrical capacitance. It is important to note that R_b is considered an ideal frequency-independent element responding the same under both dc and ac currents. An obvious example may be the case of a leaky capacitor in which the permittivity is shunted by a parallel mechanism of dc conduction. This type of situation is very common in many systems in which movements of charges, electronic or ionic, is enhanced at sufficiently elevated temperatures to give rise to dc leakage.

The change of the values of activation energy with Se content (x = 11, 14 and 17 at.%) for the investigated system is presented in Table 2. The results show that two regions of the dependence of E_1, E_2, E_{dc} and E_b on Se content. The first region lies between x = 11 and x = 14 at.%, where an increase is observed in the activation energy values with the rise in Se-content. The second region lies between x = 14 and x = 17 at.%, where a significant variation of E_1, E_2, E_{dc} and E_b is observed with the rise in Se content. This may be attributed to the effect of Se content in the positional disorder in the system.

4. Conclusion

The ac conductivity and dielectric properties of Ge Te Se glasses have been studied in a wide range of frequencies and temperatures. Analysis of the results on the basis of the correlated barrier hopping (CBH)

model reveals that the electronic conduction in Se-Te-Ge glasses takes place via bipolaron hopping. Thermal agitation induces new types of defects which take part in the single polaron-hopping conduction process.

The activation energy values for the temperature dependence of the total conductivity of the Ge-Te-Se glasses, which characterize the low temperature processes, depend on the system structure, while the high temperature activation energy values seem to be independent of the composition. This familiar behavior results from space charge build up near electrodes.

An equivalent parallel resistance-capacitance circuit to represent the impedance plot of the semicircles has been presented. The physical interpretation of the circuit is related to conduction with bulk resistance and polarization.

Electrical conductivity is affected by the structural change. The dependence of ac conductivity and dielectric constants on the Se content x can be interpreted as the effect of Se at. % on the positional disorder.

References

[1] S.R. Elliott, *Adv. Phys.*, **36**, (1987), 135.

[2] A. Hamada, M. Saito and M. Kikuchi, *Solid State Commun.,* **11**, (1972), 1409.

[3] J.S. Berkes, S.W. Ingand and W.J. Hillegas, *J. Appl. Phys.*, **42**, (1971), 4908.

[4] B.T. Kolomieto, *Phys. Status Solidi,* **7**, (1964), 713.

[5] J.E. Baurrelle, *J. Phys. Chem. Solids*, **30**, (1969), 2657.

[6] B. Roling and K. Funke, *J. Non-Cryst. Solids*, **212**, (1997), 1.

[7] Jeppe C. Dyre, *J. Appl. Phys.* **64**, (1988), 2456.

[8] S.R. Elliot, *Phil. Mag.,* **B46,** (1982), 123.

[9] J.C. Guntini and J.V. Zanchetta, *J. Non-Cryst. Solids*, **34**, (1974), 419.

[10] K. Skimakawa, *Phil. Mag.* **B46**, (1982), 123.

[11] J.R. Macdonald, *J. Non-Cryst. Solids,* **197**, (1996), 83.

[12] A.R. Long, J. McMillen, N. Balkan and S. Summerfield, *Philos. Mag.,* **B58**, (1988), 153.

[13] M. Cutroni, A. mandanici, A. Piccols and C. Tomasi, *Phil. Mag.,* **B71**, (1995), 843.

[14] K.L. Ngai, *Comments Solid State Phys.*, 9, (1979), **127**, 9, (1980), 141.